



# CHORUS

This is the accepted manuscript made available via CHORUS. The article has been published as:

## Defects in AlN as candidates for solid-state qubits

J. B. Varley, A. Janotti, and C. G. Van de Walle

Phys. Rev. B **93**, 161201 — Published 1 April 2016

DOI: [10.1103/PhysRevB.93.161201](https://doi.org/10.1103/PhysRevB.93.161201)

# Defects in AlN as candidates for solid-state qubits

J. B. Varley<sup>1,2</sup>, A. Janotti<sup>2,3</sup>, and C. G. Van de Walle<sup>2</sup>

<sup>1</sup>Lawrence Livermore National Laboratory, Livermore, CA 94550, USA

<sup>2</sup>Materials Department, University of California, Santa Barbara, CA 93106-5050 and

<sup>3</sup>Department of Materials Science and Engineering, University of Delaware, Newark, DE 19716, USA

(Dated: March 8, 2016)

We investigate point defects and defect complexes in AlN for potential applicability as single-spin centers and solid-state qubits analogous to those observed in diamond and SiC. We find that isolated anion vacancies ( $V_N$ ) meet many of the criteria for an individually-addressable quantum system, but their states are too close to the conduction-band edge. We therefore investigate how the properties can be tuned by complexing of the vacancy with substitutional impurities on neighboring lattice sites. Based on our comprehensive investigation the transition-metal dopants Ti and Zr emerge as the best candidates: they favorably substitute on the Al site and form complexes with  $V_N$  that possess the desired array of electronic and optical properties. Favorable charge and spin states, binding energies, and optical excitation energies are reported. Our results indicate that implantation of Ti or Zr into single-crystal AlN substrates can lead to the formation of individually-addressable solid-state qubits in this material.

PACS numbers: 71.55.Eq, 78.55.Cr

The rapidly growing interest in quantum-information technologies has created a need for identifying optically addressable single-spin centers that may serve as qubits. The  $NV^-$  center in diamond, which consists of a carbon vacancy ( $V_C$ ) next to a substitutional nitrogen atom ( $N_C$ ), has emerged as the prototypical deep-level solid-state qubit because of its ability to be initialized, manipulated, and measured at room temperature [1, 2]. Different polytypes of silicon carbide (SiC) have subsequently been found to also exhibit point defects that may be manipulated as room-temperature qubits [3–9], demonstrating that materials other than diamond can act as suitable hosts. It is still highly desirable to identify centers with similar characteristics in additional semiconductors or insulators for which high-quality crystal growth and processing are available.

In this article we investigate AlN as a candidate host material. AlN meets the requirements [4] to act as a host for qubit centers: it has a very large band gap (6.12 eV [10]), which suppresses coupling between defect levels in the band gap and bulk states, and a very small spin-orbit splitting (19 meV [11]), which enhances qubit-state lifetime. High-quality crystal growth [12–14] and doping techniques [15] have been developed. A slight drawback is that its host elements have nonzero nuclear spin [4]; however, spin-bath effects can be brought under control with appropriate pulsing and polarization techniques [16]. AlN is thus an attractive host material, and our aim is to identify suitable single-spin centers.

We will show that defect theory points to complexes between nitrogen vacancies ( $V_N$ ) and donor defects as attractive qubit candidates. The quantitative details are addressed with cutting-edge first-principles calculations based on density functional theory (DFT) with a hybrid functional. In particular, we conduct a comprehensive investigation of group-IV impurities and their complexes with  $V_N$ . Transition-metal impurities such as Ti or Zr emerge as excellent candidates to form complexes with  $V_N$  that show outstanding promise as qubits.

Point defects induce levels within the band gap of a semiconductor that, when appropriately occupied with electrons, can give rise to controllable quantum states. Vacancies, in particular, provide suitable states that are “atomic-like” due to the concentration of their wavefunction within a small spatial volume. The electronic structure of a tetrahedrally bonded material such as AlN can be understood within molecular orbital (or tight-binding) theory in terms of interactions between  $sp^3$  hybrid orbitals, with bonding (antibonding) combinations giving rise to the valence (conduction) bands. The removal of a host atom leads to “dangling bonds” (DBs) (hybrid orbitals on the neighboring atoms) that interact and split into a symmetric  $a_1$  state and three  $t_2$  states. Suitable arrangement of electrons in these states can give rise to spin configurations suitable for use as a solid-state qubit [4]. The electron occupation (which determines the charge state of the defect) is determined by the Fermi level in the material, which in turn can be controlled by doping. The energetic position and ordering of the states, which determines the spin, can also be manipulated, for instance by positioning suitable impurities near the vacancy. In analogy with the prototype  $NV^-$  center in diamond and the  $(V_{Si}-V_C)^0$  center in 4H-SiC [3, 7], a triplet ( $S=1$ ) ground state is desirable, although recent experiments have identified that a quadruplet ( $S=3/2$ ) state (as in  $V_{Si}^-$  in SiC) can also be suitable [9].

Vacancies in AlN can form on the cation or anion sites. In a cation vacancy, the DBs are anion-derived and hence lie within the lower half of the band gap [17]. Ensuring that the resulting defect levels are not too close to the valence-band maximum (VBM) and sufficiently isolated from the bulk states [4] may require additional engineering, as recently explored for a  $V_{Al}-O_N$  complex [18]. However, manipulating the charge and spin states in such cation-vacancy-related centers would require the Fermi level to lie below mid-gap, which is challenging in AlN. Indeed,  $p$ -type conductivity in AlN has not been demonstrated [19].

The natural tendency of AlN towards Fermi-level positions

in the upper part of the gap (as evidenced by the feasibility of  $n$ -type doping [15, 20, 21]) renders defect centers based on anion vacancies more promising. Here, cation DBs interact to form the defect states. Cation DBs lie in the upper part of the gap [17], and hence the  $t_2$  states may be too close to the conduction-band minimum (CBM). As with the cation vacancy, defect engineering can push the  $t_2$  levels deeper into the gap, for instance by applying strain, by alloying the host with a larger band gap material (such as BN), or by complexing with an adjacent impurity. We will focus on the latter, in particular on donor dopants that stabilize defect levels in a complex. Complex formation is actually facilitated by the Coulomb attraction between positively charged donors and the  $V_N^-$  (which is negatively charged when the Fermi level is in the upper part of the gap, a natural consequence of donor doping).

We will investigate the quantitative details of this scheme by performing advanced first-principles calculations based on the HSE06 screened hybrid functional [22, 23]. This methodology was previously very successful in describing the properties of analogous deep center qubit candidates such as the  $NV^-$  center in diamond and the divacancy in SiC.[3–9] In particular, we investigate a number of group-IV impurities and their complexes with  $V_N$ , finding that most of them do not have any significant effect on the positions of the  $t_2$ -derived defect levels within the bandgap. The exceptions are transition metals such as Ti or Zr, which strongly affect the position and nature of the vacancy levels and lead to favorably positioned localized states within the band gap. Specifically, we will find the neutral  $(Ti_{Al}V_N)^0$  and  $(Zr_{Al}V_N)^0$  complexes to be stable for a wide range of conditions and to exhibit  $S=1$  spin configurations well suited for application in solid-state qubits. The results for Ti in SiC in Ref. 24 support the notion that our hybrid functional approach yields reliable results for Ti and Zr-related defects in AlN.

Defect formation energies ( $E^f$ ) are key quantities from which we can derive impurity and defect concentrations, the stability of different charge states, and the related electronic transition levels [25]. Since the spin states depend on the charge state,  $E^f$  also determines whether a given defect will occur in a desired spin configuration. The formation energy of the  $V_N$  in AlN is given by

$$E^f[V_N^q] = E_{\text{tot}}[V_N^q] - E_{\text{tot}}[\text{AlN}] + \frac{1}{2}E_{\text{tot}}[\text{N}_2] + \mu_N + q\varepsilon_F + \Delta_q, \quad (1)$$

where  $E_{\text{tot}}[V_N^q]$  and  $E_{\text{tot}}[\text{AlN}]$  represent the total energy of the supercell containing a vacancy in charge state  $q$ , and that of a perfect crystal in the same supercell. The Fermi level  $\varepsilon_F$  represents the chemical potential for electrons, which is referenced to the VBM and ranges over the band gap up to the CBM. The chemical potential ( $\mu_N$ ) represents the energy of the reservoir with which N atoms are exchanged and reflects the experimental conditions; it varies between N-rich (Al-poor) and N-poor (Al-rich) extremes, with bounds set by the calculated formation enthalpy of AlN ( $\mu_{Al} + \mu_N = \Delta H[\text{AlN}] = -3.18$  eV). Lastly, the  $\Delta_q$  term represents the charge-dependent finite-size

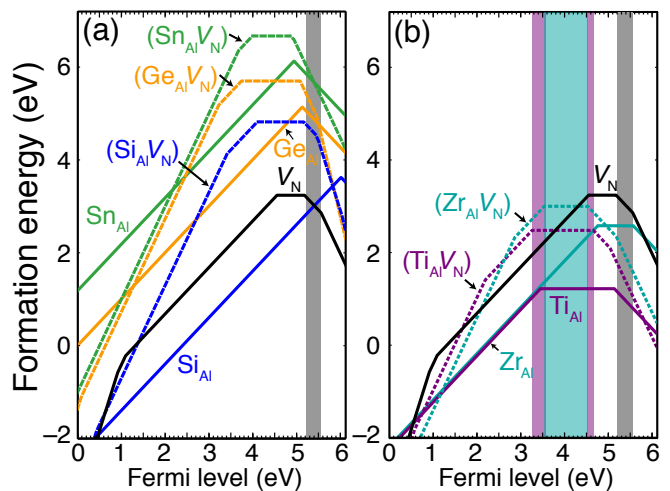


FIG. 1. (Color online) Formation energies of the isolated  $V_N$ , various dopant impurities substituting on the Al site, and complexes in AlN, for Al-rich conditions. (a) Group-IVA impurities (Si, Ge, Sn); (b) Group-IVB impurities (Ti and Zr). Only the lowest-energy configurations of the complexes are included, as described in the text. Shaded regions indicate the Fermi-level values for which an  $S=1$  state is favored for the isolated  $V_N$  (grey), for the  $(Ti_{Al}V_N)^0$  complex (purple), and for the  $(Zr_{Al}V_N)^0$  complex (teal).

correction [26]. Similar expressions apply to impurities or dopants, whose chemical potentials may be coupled to those of the host elements, as detailed in the Supplemental Material [23].

Formation energies such as Eq. (1) can be used to determine defect concentrations when conditions are sufficiently close to equilibrium; non-equilibrium processes such as ion implantation can result in higher concentrations. Even in the latter case, formation energies can provide useful information about the relative stability of various configurations, about binding energies for complexes, about what charge and spin states a given defect will adopt for a given Fermi-level position, and about the position of its defect levels in the band gap.

Formation energies of the  $V_N$  and various dopants are shown in Fig. 1 for Al-rich conditions [23]. The vacancy can assume many different charge states, ranging from +3 for  $\varepsilon_F$  at the VBM to  $-2$  for  $\varepsilon_F$  at the CBM. The desired high-spin states ( $S=1$  or  $S=3/2$ ) occur only for charge state  $(-1$  and  $-2)$  that have high formation energies (even under the most favorable Al-rich conditions), making it unlikely that vacancies would form spontaneously. This is not an obstacle, however, since vacancies can readily be produced by irradiation or ion implantation, as is common practice for the  $NV^-$  center in diamond.

We find that the low-spin configurations of  $V_N$  ( $S=0$  or  $1/2$ ) are only  $\sim 0.1$  eV higher in energy than the  $S=1$  or  $3/2$  configurations, indicating a potential sensitivity to spin-flips from external perturbations. Another drawback is that the states associated with the excited configuration of the isolated  $V_N^-$  and  $V_N^{-2}$  centers are very close to the CBM, as illustrated in

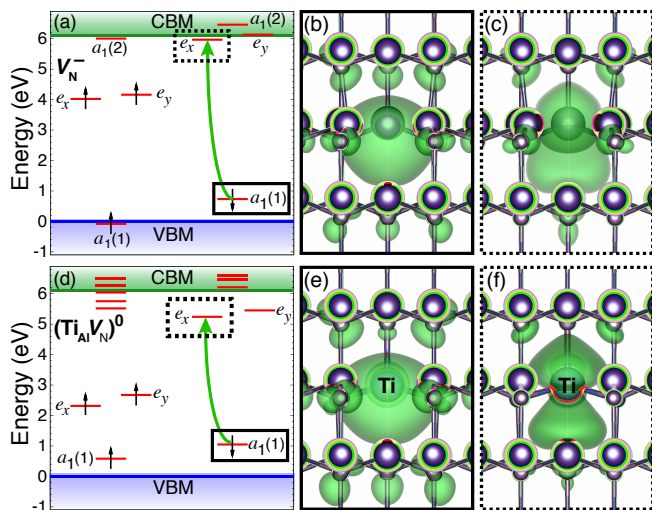


FIG. 2. (Color online) Defect-level diagrams (DLDs) for (a) an isolated negatively charged nitrogen vacancy  $V_N^{-1}$  and (b) a  $(Ti_{Al}V_N)^0$  complex in AlN, showing the location and occupancy of the single-particle defect states within the band gap. The arrows indicate the spin-conserving internal transition from the occupied  $a_1(1)$  state (solid box) to the unoccupied  $e$  state (dashed box) in the spin-minority channel. To the right are charge-density isosurfaces depicting wave functions for the single-particle states involved in these transition: (b)  $a_1(1)$  state of  $V_N^{-1}$ ; (c)  $e_x$  state of  $V_N^{-1}$ ; (e)  $a_1(1)$  state of  $(Ti_{Al}V_N)^0$  (f)  $e_x$  state of  $(Ti_{Al}V_N)^0$ . The isosurfaces are displayed at 10% of their maximum value.

the defect level diagram (DLD) of Fig. 2(a). The DLD for the  $V_N^{-2}$  is nearly identical, but with the spin-majority  $a_1(2)$  state occupied to give the  $S=3/2$  state. Along with the small energy difference between the high- and low-spin states, this proximity could be an additional source of decoherence due to coupling with the bulk conduction-band states that could limit the effectiveness of the isolated  $V_N$  in AlN as a viable qubit candidate. We therefore explore how the properties of the spin center can be engineered through complexing with impurities.

Si, Ge, and Sn prefer the substitutional Al site in AlN, and act as donors. In particular, Si is a successful  $n$ -type dopant in AlN [15, 20]. The formation energies of Si, Ge, and Sn are plotted in Fig. 1(a). All three of these impurities exhibit DX-like behavior; i.e., for Fermi levels high in the band gap they become more stable in a negative charge state (and thus act as acceptors), accompanied by a large lattice relaxation. If these dopants are incorporated in high concentrations (exceeding the concentration of any other defect or impurity), charge neutrality will pin the Fermi level at the  $\varepsilon(+/-)$  transition level, which occurs at 0.12 eV below the CBM for Si, 0.99 eV for Ge, and 1.18 eV below for Sn. These transition levels are in good agreement with experimental and theoretical data where available [20, 27].

We now examine the complexes formed between the group-IVA impurities and  $V_N$ , whose formation energies are also included in Fig. 1(a). The formation energy of the complexes is

quite high for Fermi-level positions that lead to desirable spin states. However, as already noted,  $V_N$  are likely to be introduced by implantation or irradiation; based on reported migration barriers for  $V_N$  in GaN ( $\sim 2.6$ – $4.3$  eV) [28–30] we estimate a temperature in excess of  $500^\circ\text{C}$  is needed to drive the formation of complexes via  $V_N$  diffusion. The complexes are stable in charge states ranging from  $+2$  to  $-3$ . Unfortunately, the process of complex formation turns out to destabilize the desired  $S=1$  and  $S=3/2$  states. The local lattice relaxations favor low-spin ground states, and therefore these complexes between  $V_N$  and Group-IVA donors do not serve as suitable NV-center analogs.

We therefore turn to an exploration of Group-IVB dopants, in particular the transition metals Ti and Zr. As seen in Fig. 1(b) these impurities can assume  $+1$ ,  $0$  and  $-1$  charge states and have very modest formation energies when incorporated on the Al site for both Al-rich and N-rich conditions [23]. Incorporation on the N site is highly energetically unfavorable.  $Ti_{Al}$  and  $Zr_{Al}$  can therefore easily be incorporated during growth, and if they are present in concentrations higher than those of other impurities or native defects, they will also determine the location of the Fermi level: if additional impurities/defects are predominantly donor-like,  $\varepsilon_F$  will be pinned at the  $\varepsilon(0/-)$  level of the transition-metal impurity (2.67 eV below the CBM for  $Ti_{Al}$  and 1.37 below the CBM for  $Zr_{Al}$ ); if additional impurities are predominantly acceptor-like,  $\varepsilon_F$  will be pinned at the  $\varepsilon(+/0)$  level of the transition-metal impurity (0.99 eV below the CBM for  $Ti_{Al}$  and 0.53 eV below the CBM for  $Zr_{Al}$ ).

Complexes between Ti and Zr and the  $V_N$  are also included in Fig. 1(b). The neutral complexes are stable in the  $S=1$  state, highlighted by the shaded regions in Fig. 1(b): from 2.87 to 1.46 eV below the CBM for  $(Ti_{Al}V_N)^0$  and from 2.58 to 1.59 eV below the CBM for  $(Zr_{Al}V_N)^0$ . The  $-1$  charge state of the complexes favors a low-spin  $S=1/2$  configuration, making it uninteresting as a qubit candidate. These numbers actually indicate a very favorable situation in the case of Ti: as noted above, in the presence of additional donor-like impurities/defects, a high concentration of  $Ti_{Al}$  will pin  $\varepsilon_F$  at 2.67 eV below the CBM, within the stability window of neutral  $(Ti_{Al}V_N)^0$  ( $S=1$ ). With Zr the situation is not as advantageous: stabilizing the  $(Zr_{Al}V_N)^0$  complex would require additional doping measures to fix the Fermi level.

In terms of their spin configurations, we find that the level structure of the complexes is advantageously distanced from the CBM as seen from the DLD of the  $(Ti_{Al}V_N)^0$  in Fig. 2(b). We find that the symmetry of the localized defect states of the complexes is preserved while the position of the higher-lying  $e$  states is lowered relative to the analogous levels for the isolated  $V_N$ . This suggests the  $(Ti_{Al}V_N)^0$  and  $(Zr_{Al}V_N)^0$  complexes could support quantum states that are less prone to unwanted coupling with the delocalized conduction band states.

It is also important to assess how stable the complexes are with respect to dissociation. The binding energy of the  $(Ti_{Al}V_N)^0$  complex can be estimated relative to constituents

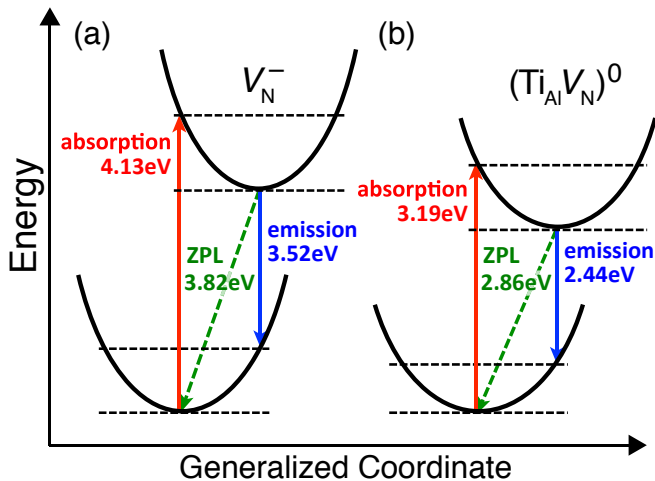


FIG. 3. (Color online) Configuration coordinate diagram of the spin-conserving triplet excitations for (a) the  $V_N^-$  and (b) the  $(\text{Ti}_{\text{Al}}V_N)^0$  complex in AlN. The absorption, emission, and zero-phonon line (ZPL) energies are for excitations in the spin-minority channel as shown in Figs. 2(a) and (d). Axes are not to scale.

that obey charge neutrality. With respect to  $\text{Ti}_{\text{Al}}^-$  and  $V_N^+$  the binding energy is 2.6 eV; with respect to  $\text{Ti}_{\text{Al}}^+$  and  $V_N^-$ , 3.7 eV; and with respect to  $\text{Ti}_{\text{Al}}^0$  and the  $V_N^0$ , 2.0 eV. These numbers indicate that, once formed, the complexes will be stable. For the Zr-containing complexes, we find similarly large binding energies in excess of 2 eV.

Having addressed the formation, stability, and spin state of the complexes, we now examine the optical excitation energies. Results are summarized in Table I, which also contains values for the isolated  $V_N$ . We obtain the optical energies using a configuration-coordinate diagram analysis as illustrated in Fig. 3 and schematically included in Fig. 2 for the intra-defect transitions of the  $V_N^-$  and  $(\text{Ti}_{\text{Al}}V_N)^0$ . The calculated absorption energies range from 2.8 eV to 4.2 eV and have zero-phonon (ZPL) lines from 2.4 to 3.8 eV. These values are much larger than those for other deep-center qubits such as the  $NV^-$  center in diamond (ZPL  $\sim 2$  eV) or complexes in SiC (ZPL  $\sim 1$  eV) [6, 7, 9]. This distinction indicates that qubits in AlN may provide functionality in the blue or UV region of the spectrum, compared to red or infrared excitations for qubits in diamond and SiC.

Lastly we evaluate the isolation of the excited quantum states by combining the charge-state transition levels with the calculated optical excitation energies. For the example of the isolated  $V_N^-$ , we can estimate the position of the optically-excited state by adding the ZPL (3.8 eV) to the  $\epsilon(0/-)$  level ( $\sim 1.0$  eV below the CBM), finding that an electron would be excited to a state  $\sim 2.8$  eV above the CBM. Such an excitation could occur in an Auger-like process where the electron escapes to the conduction band, as was shown for the  $NV^-$ -to- $NV^0$  transition in diamond [31]. For the  $(\text{Ti}_{\text{Al}}V_N)^0$ , this same analysis leads to an excited state at  $\sim 0.9$  eV below the CBM, indicating this state would be less prone to decoherence.

Table I also lists the energies required to ionize the defects by promoting an electron to the CBM rather than forming an intra-defect photo-excited state of the deep center. These energies provide an additional measure of the optical isolation of the defect centers, representing the energy necessary to couple the defect to the bulk states by promoting an electron to the CBM. As seen in the DLDs of Fig. 2, the lowest-energy excitation of this type would correspond to promoting the highest-lying electron in the spin-majority channel [e.g., from the occupied  $e_y$  state for the case of the  $V_N^-$  in Fig. 2(a)]. Another transition corresponds to the excitation of the highest-occupied spin-minority electron to the CBM. The difference in energy between this transition and the intra-defect transition is a good metric of how isolated the defect states are from the CBM. These differences are gratifyingly large in the case of the  $(\text{Ti}_{\text{Al}}V_N)$  and  $(\text{Zr}_{\text{Al}}V_N)$  complexes.

In summary, we have found that  $V_N$ -related centers in AlN can lead to viable deep-center qubits that exhibit properties similar to the  $NV^-$  center in diamond. Based on a comprehensive study of Group-IV impurities, Ti and Zr were found to be the most promising dopants that can be stabilized in  $(\text{Ti}_{\text{Al}}V_N)^0$  and  $(\text{Zr}_{\text{Al}}V_N)^0$  complexes with  $V_N$  that possess a high-spin ( $S = 1$ ) ground state. The optical signatures associated with these complexes confirm that they could provide robust solid-state qubit candidates in the blue or UV.

The authors thank A. Alkauskas, J. R. Weber, L. Gordon, J. Lyons, W. F. Koehl, and D. Awschalom for useful discussions. This work was performed in part under the auspices of the U.S. Department of Energy at Lawrence Livermore National Laboratory under Contract DE-AC52-07NA27344. Additional support was provided by NSF under Grant No. DMR-143485. Computational resources were provided by the Center for Scientific Computing at the CNSI and MRL (an NSF MRSEC, DMR-1121053) (NSF CNS-0960316), and by the Extreme Science and Engineering Discovery Environment (XSEDE), which is supported by NSF under Grant No. ACI-1053575.

- 
- [1] B. B. Buckley, G. D. Fuchs, L. C. Bassett, and D. D. Awschalom, *Science* **330**, 1212 (2010).
  - [2] P. Neumann, J. Beck, M. Steiner, F. Rempp, H. Fedder, P. R. Hemmer, J. Wrachtrup, and F. Jelezko, *Science* **329**, 542 (2010).
  - [3] A. Gali, A. Gällström, N. T. Son, and E. Janzén, *Mater. Sci. Forum* **645**, 395 (2010).
  - [4] J. R. Weber, W. F. Koehl, J. B. Varley, A. Janotti, B. B. Buckley, C. G. Van de Walle, and D. D. Awschalom, *Proc. Natl. Acad. Sci. USA* **107**, 8513 (2010).
  - [5] J. R. Weber, W. F. Koehl, J. B. Varley, A. Janotti, B. B. Buckley, C. G. Van de Walle, and D. D. Awschalom, *J. Appl. Phys.* **109**, 102417 (2011).
  - [6] L. Gordon, J. R. Weber, J. B. Varley, A. Janotti, D. D. Awschalom, and C. G. Van de Walle, *MRS Bull.* **38**, 802 (2013).
  - [7] W. F. Koehl, B. B. Buckley, F. J. Heremans, G. Calusine, and

TABLE I. Calculated optical excitation energies (absorption, emission, and zero-phonon line, ZPL) associated with the spin-conserving excitations [see Fig. 3(a) and (d)] of isolated  $V_N$  and  $(Ti_{Al}V_N)$  and  $(Zr_{Al}V_N)$  complexes in AlN. Competing channels that ionize the centers by excitation to the conduction band are also described. All values are in eV.

Center	$D^q + \hbar\omega \rightarrow D^q$			$D^q + \hbar\omega \rightarrow D^{q+1} + e^- _{CBM}$					
	Spin-conserving excitation: $S \rightarrow S$			Spin-minority excitation: $S \rightarrow S + 1/2$			Spin-majority excitation: $S \rightarrow S - 1/2$		
	Absorption	ZPL	Emission	Absorption	ZPL	Emission	Absorption	ZPL	Emission
$V_N^-$	4.13	3.82	3.52	4.84	4.13	3.49	1.62	0.95	0.31
$V_N^{-2}$	4.17	3.83	3.52	4.36	3.70	3.12	1.20	0.62	0.04
$(Ti_{Al}V_N)^0$	3.19	2.86	2.44	5.16	4.43	3.92	3.34	2.76	2.25
$(Zr_{Al}V_N)^0$	2.83	2.36	1.91	4.97	4.29	3.78	3.07	2.62	2.11

- D. D. Awschalom, *Nature* **479**, 84 (2012).
- [8] A. L. Falk, B. B. Buckley, G. Calusine, W. F. Koehl, V. V. Dobrovitski, A. Politi, C. A. Zorman, P. X. L. Feng, and D. D. Awschalom, *Nat. Comm.* **4**, 1819 (2013).
- [9] M. Widmann, S.-Y. Lee, T. Rendler, N. T. Son, H. Fedder, S. Paik, L.-P. Yang, N. Zhao, S. Yang, I. Booker, A. Denisenko, M. Jamali, S. A. Momenzadeh, I. Gerhardt, T. Ohshima, A. Gali, E. Janzén, and J. Wrachtrup, *Nat. Mater.* **14**, 164.
- [10] J. Li, K. B. Nam, M. L. Nakarmi, J. Y. Lin, H. X. Jiang, P. Carrier, and S.-H. Wei, *Appl. Phys. Lett.* **83**, 5163 (2003).
- [11] S.-H. Wei and A. Zunger, *Appl. Phys. Lett.* **69**, 2719 (1996).
- [12] J. Carlos Rojo, G. A. Slack, K. Morgan, B. Raghathamachar, M. Dudley, and L. J. Schowalter, *J. Cryst. Growth* **231**, 317 (2001).
- [13] M. Bickermann, B. M. Epelbaum, O. Filip, P. Heimann, S. Nagata, and A. Winnacker, *Phys. Status Solidi C* **7**, 21 (2010).
- [14] H. Okumura, T. Kimoto, and J. Suda, *Appl. Phys. Express* **4**, 025502 (2011).
- [15] Y. Taniyasu, M. Kasu, and T. Makimoto, *Appl. Phys. Lett.* **85**, 4672 (2004).
- [16] G. de Lange, Z. H. Wang, D. Ristè, V. V. Dobrovitski, and R. Hanson, *Science* **330**, 60 (2010).
- [17] W. A. Harrison, *Electronic Structure and the Properties of Solids: The Physics of the Chemical Bond* (Dover Publications, Incorporated, 2012).
- [18] Y. Tu, Z. Tang, X. G. Zhao, Y. Chen, Z. Q. Zhu, J. H. Chu, and J. C. Fang, *Appl. Phys. Lett.* **103**, 072103 (2013).
- [19] J. L. Lyons, A. Janotti, and C. G. Van de Walle, *Phys. Rev. Lett.* **108**, 156403 (2012).
- [20] N. T. Son, M. Bickermann, and E. Janzén, *Appl. Phys. Lett.* **98**, 092104 (2011).
- [21] L. Gordon, J. B. Varley, J. L. Lyons, A. Janotti, and C. G. Van de Walle, *Phys. Status Solidi RRL* **9**, 462 (2015).
- [22] J. Heyd, G. E. Scuseria, and M. Ernzerhof, *J. Chem. Phys.* **118**, 8207 (2003); **124**, 219906 (2006).
- [23] Details of the calculations and formation energies shown for both N-rich and Al-rich conditions are included in the Supplementary Material.
- [24] V. Ivády, I. A. Abrikosov, E. Janzén, and A. Gali, *Phys. Rev. B* **87**, 205201 (2013).
- [25] C. Freysoldt, B. Grabowski, T. Hickel, J. Neugebauer, G. Kresse, A. Janotti, and C. G. Van de Walle, *Rev. Mod. Phys.* **86**, 253 (2014).
- [26] C. Freysoldt, J. Neugebauer, and C. G. Van de Walle, *Phys. Rev. Lett.* **102**, 016402 (2009); *Phys. Status Solidi B* **248**, 1067 (2010).
- [27] L. Gordon, J. L. Lyons, A. Janotti, and C. G. Van de Walle, *Phys. Rev. B* **89**, 085204 (2014).
- [28] A. Uedono, K. Ito, H. Nakamori, K. Mori, Y. Nakano, T. Kachi, S. Ishibashi, T. Ohdaira, and R. Suzuki, *J. Appl. Phys.* **102** (2007).
- [29] F. Tuomisto, V. Ranki, D. C. Look, and G. C. Farlow, *Phys. Rev. B* **76**, 165207 (2007).
- [30] S. Limpijumong and C. G. Van de Walle, *Phys. Rev. B* **69**, 035207 (2004).
- [31] P. Siyushev, H. Pinto, M. Vörös, A. Gali, F. Jelezko, and J. Wrachtrup, *Phys. Rev. Lett.* **110**, 167402 (2013).